Supplementary Materials

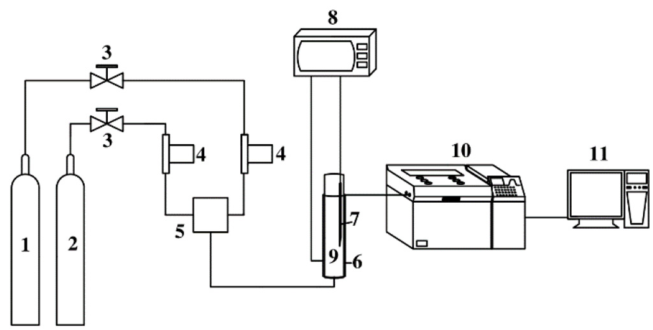

Fig. S1. CO_2 dynamic adsorption unit. (1-argon cylinder; 2-CO_2 cylinder; 3-gas pressure relief valve; 4-mass flow controller; 5-gas mixer; 6-heating mantle; 7-temperature probe; 8-temperature controller; 9-reactor; 10-gas chromatography; 11-gas chromatography work station)

Table S1. Textural Properties of Mg-MOF-74 and Mg-MOF-nNH_2

Samples	Textural properties			
	BET surface area (m^2/g)	Average pore size (nm)	Total pore volume (cm^3/g)	Micropore volume (cm^3/g)
Mg-MOF-74	1122.47	2.00	0.57	0.43
Mg-MOF-1/10NH_2	1056.34	2.31	0.61	0.41
Mg-MOF-1/8NH_2	924.19	2.32	0.54	0.46
Mg-MOF-1/6NH_2	692.16	2.45	0.42	0.27
Mg-MOF-1/4NH_2	515.36	3.57	0.46	0.21

Table S2. Parameters Values of Lagergen's Pseudo-first-order Kinetics Model and Ho's Pseudo-second-order Kinetics Model of Mg-MOF-1/8NH_2

Temperature/K	pseudo-first-order kinetics			pseudo-second-order kinetics			Avrami			
	q_e mmol/g	k_1 min^{-1}	R^2	q_e mmol/g	k_2 min^{-1}	R^2	q_e mmol/g	k_a min^{-1}	n	R^2
303K	4.04	0.08	0.998	5.33	0.01	0.996	4.00	0.08	1.02	0.999
313K	3.06	0.09	0.996	3.95	0.02	0.998	3.15	0.08	0.92	0.999
323K	2.37	0.18	0.969	2.72	0.08	0.991	2.47	0.17	0.75	0.983

Table S3. Parameters Values of Langmuir, Freundlich Isotherms Models of Mg-MOF-1/8NH_2

Temperature/K	Langmuir			Freundlich		
	q_m mmol/g	K_L min^{-1}	R^2	K_f	$1/n$	R^2
303K	6.16	0.017	0.971	0.32	0.55	0.964
313K	4.51	0.020	0.943	0.31	0.51	0.935
323K	4.02	0.021	0.959	0.25	0.52	0.952

Table S4. Comparison of Mg-MOF-74 and Mg-MOF-1/8NH_2 CO_2 Adsorption Capacity

Adsobents	303K C_0 = 100%	313K C_0 = 100%	323K C_0 = 100%
Mg-MOF-74	3.57mmol/g	2.53mmol/g	1.83 mmol/g
Mg-MOF-1/8NH_2	3.90 mmol/g	3.00 mmol/g	2.64 mmol/g

Table S5. The Parameters of Thermodynamics

Adsobents	CO_2 thermodynamic parameters				
	△G(kJ/mol)			△H (kJ/mol)	△S (J/mol)
	303K	313K	323K		
Mg-MOF-1/8NH_2	-10.22	-10.27	-10.32	-8.64	5.2

Table S6. The Parameters of Equivalent Heat of Adsorption

q_a(mmol/g)	1	1.3	1.6	1.9	2.2	2.5
R^2	0.998	0.997	0.993	0.991	0.989	0.989
slope	-1635.8	-1916.6	-2204.1	-2561.9	-3026.5	-3611.4
Q_{st}	27.20	31.87	36.65	42.60	50.32	60.05

Table S7. Fitted Parameters of the Deactivation Model of Mg-MOF-1/8NH_2 at Different Temperatures

T	k_0 M/Q	k_0 (cm_3 min^{-1} g^{-1})	k_d(min^{-1})	R^2
303K	2.77	1.11 × 10^2	0.37	0.992
313K	3.26	1.30 × 10^2	0.48	0.995
323K	1.89	0.76 × 10^2	0.49	0.982

Table S8. Fitted Parameters of the Deactivation Model of Mg-MOF-1/8NH_2 at Different Temperatures

T	k_0M/Q	k_0 (cm^3 min^{-1} g^{-1})	k_d(min^{-1})	R^2
303K	3.78	1.51 × 10^2	0.74	0.998
313K	2.21	0.88 × 10^2	0.52	0.985
323K	1.81	0.72 × 10^2	0.57	0.962

Table S9. Fitted Parameters of the Deactivation Model of Mg-MOF-74 at Different Concentrations

C_0	k_0M/Q	k_0 (cm^3 min^{-1} g^{-1})	k_d(min^{-1})	R^2	q(mmol/g)
10%	3.78	1.512 × 10^2	0.74	0.998	1.08
20%	4.06	1.624 × 10^2	0.863	0.999	1.49
30%	6.11	2.444 × 10^2	1.49	0.996	1.72
50%	2.55	1.020 × 10^2	1.02	0.988	2.21

Table S10. Fitted Parameters of the Deactivation Model of Mg-MOF-1/8NH_2 at Different Concentrations

C_0	k_0M/Q	k_0 (cm^3 min^{-1} g^{-1})	k_d(min^{-1})	R^2	q(mmol/g)
10%	2.81	1.124×10^2	0.38	0.959	1.27
20%	2.76	1.104×10^2	0.45	0.914	1.82
30%	1.88	0.752×10^2	0.54	0.988	2.11
50%	1.94	0.776×10^2	0.63	0.992	3.31

Table S11. CO_2 Adsorption of Other Material Capacity

Adsorbents	Adsorption conditions		CO_2 adsorption (mmol/g)	Ref
	Pressure (bar)	Adsorption temperature (K)		
Mg-MOF-1/8NH_2	1	303	3.9	this work
Mg-MOF-74	1	303	3.57	this work
AC Norit RB1	1	294.2	2.456	[1]
anthracite-based AC	1	303	1.38	[2]
Zeolite 13X	1	298	4.66	[3]
NaM	1	298	2.95	[4]
N-rich porous carbon	1	298	2.3	[5]
Mesoporous alumina	1	298	1.2	[6]
MIL-125	1	298	2.18	[7]
MIL-101(Cr)	1	298	1.22	[8]
UPC-106	1	298	2.42	[9]
MOF-177	1	298	0.77	[10]
Fe-BTT	1	298	3.07	[11]
HKUST-1	1	298	4.16	[12]

References

1. Vaart R, Huiskes C, Bosch H, et al. Single and mixed gas adsorption equilibria of carbon dioxide/methane on activated carbon. *Adsorption* 2000;6:311-323.
2. Maroto-Valer MM, Tang Z, Zhang Y. CO_2 capture by activated and impregnated anthracites. *Fuel Process Technol.* 2005;86:1487-1502.
3. Cavenati S, Grande CA, Rodrigues, et al. Adsorption equilibrium of methane, carbon dioxide, and nitrogen on zeolite 13X at high pressures. *J. Chem. Eng. Data* 2004;49:1095-1101.
4. ChouHary VR, Mayadevi S, Singh AP. Sorption isotherms of methane, ethane, ethene and carbon dioxide on NaX, NaY and Na-mordenite zeolites. *J. Chem. Soc.* 1995;91:2935–2944.
5. Chao C, Kim J, Ahn W S. Efficient carbon dioxide capture over a nitrogen-rich carbon having a hierarchical micro-mesopore structure. *Fuel* 2012;95:360-364.
6. Chen C, Ahn WS. CO_2 capture using mesoporous alumina prepared by a sol–gel process. *Chem. Eng. J.* 2011;166:646-651.
7. Kim SN, Kim J, Kim HY, et al. Adsorption/catalytic properties of MIL-125 and NH_2-MIL-125. *Catal. Today* 2013;204:85-93.
8. Chen C, Feng NJ, Guo QR, et al. Surface engineering of a chromium metal-organic framework with bifunctional ionic liquids for selective CO_2 adsorption: Synergistic effect between multiple active sites. *J. Colloid. Interface. Sci.* 2018;521:91-101.
9. Fan W, Wang X, Liu X, et al. Regulating C_2H_2 and CO_2 Storage and separation through pore environment modification in a microporous Ni-MOF. *ACS Sust. Chem. Eng.* 2018;7:2134-2140.
10. Millward A R, Yaghi O M. Metal-organic frameworks with exceptionally high capacity for storage of carbon dioxide at room temperature. *J. Am. Chem. Soc.* 2005;127:17998-17999.
11. Hon LC, Babarao R, Hill MR. A route to drastic increase of CO_2 uptake in Zr metal organic framework UiO-66. *Chem. Commun.* 2013;49:3634-3636.
12. Chong C, Li B, Zhou L, et al. Synthesis of hierarchically structured hybrid materials by controlled self-assembly of metal–organic framework with mesoporous silica for CO_2 adsorption. *ACS Appl. Mater. Inter.* 2017;9:23060-23071.